Journal of Biomolecular NMR, **19:** 231–241, 2001.
KLUWER/ESCOM

Improved NMR spectra of a protein–DNA complex through rational mutagenesis and the application of a sensitivity optimized isotope-filtered NOESY experiment

Junji Iwahara, Jonathan M. Wojciak & Robert T. Clubb*
Department of Chemistry and Biochemistry and UCLA-DOE Laboratory of Structural Biology and Genetics, University of California at Los Angeles, 405 Hilgard Ave, Los Angeles, CA 90095, U.S.A.

Received 16 August 2000; Accepted 24 November 2000

Key words: chemical exchange broadening, isotope-filtered experiment, mutation, protein complex

Abstract

The NMR spectra of the complex between the DNA-binding domain of the Dead ringer protein (DRI-DBD, Gly262-Gly398) and its DNA binding site (DRI-DBD:DNA, 26 kDa) have been optimized by biochemical and spectroscopic means. First, we demonstrate the utility of a modified 2D [F1,F2] ^{13}C-filtered NOESY experiment that employs a $^{1}J_{HC}$ versus chemical shift optimized adiabatic ^{13}C inversion pulse [Zwahlen, C. et al. (1997) *J. Am. Chem. Soc.*, **119**, 6711–6721]. The new sequence is shown to be more sensitive than previously published pulse schemes (up to 40% in favorable cases) and its utility is demonstrated using two protein–DNA complexes. Second, we demonstrate that the targeted replacement of an interfacial aromatic residue in the DRI-DBD:DNA complex substantially reduces line broadening within its NMR spectra. The spectral changes are dramatic, salvaging a protein–DNA complex that was originally ill suited for structural analysis by NMR. This biochemical approach is not a general method, but may prove useful in the spectral optimization of other protein complexes that suffer from interfacial line broadening caused by dynamic changes in proximal aromatic rings.

Introduction

The structure determination of macromolecular complexes by NMR spectroscopy remains a challenging problem, since several factors conspire to degrade the quality of the NMR data (e.g. increased molecular weights, increased spectral complexities, and line broadening caused by chemical exchange). A typical approach used to characterize these structures involves uniform labeling of one of the components with ^{15}N and ^{13}C, while the second component remains unlabeled. This enables the collection of isotope filtered and edited NMR data to define the conformation of the unlabeled and labeled components of the complex, respectively (reviewed in Clore and Gronenborn, 1998). It also makes it possible to visualize intermolecular NOEs by selecting for magnetization that is transferred between protons on the unlabeled component and protons attached to labeled heteroatoms. In these studies it is critical that the signal intensities of the protons within the molecular interface be sufficiently strong so as to enable both their atom-specific assignment and the collection of intra- and intermolecular NOEs to decipher the structural basis of recognition.

We have been attempting to solve the solution structure of the complex formed between the DNA-binding domain of the Dead ringer protein (DRI-DBD, Gly262-Gly398) and its DNA binding site (DRI-DBD:DNA, 26 kDa), but have been hindered by the weak intensities of proton signals within its interface. The Dead ringer protein from *Drosophila melanogaster* is a transcriptional regulatory protein required for early embryonic development, and it is the founding member of a large family of proteins that interact with DNA through a highly conserved domain called the AT-rich interaction domain (ARID)

*To whom correspondence should be addressed. E-mail: rclubb@mbi.ucla.edu

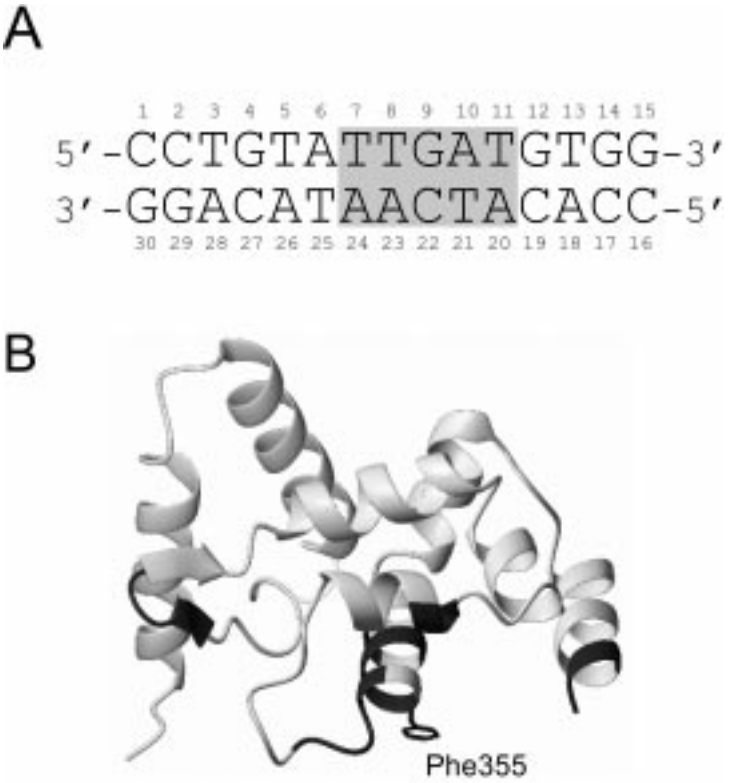

Figure 1. The components of the DRI-DBD:DNA complex. (A) The sequence of the 15-bp DNA fragment in the DRI-DBD:DNA complex. The majority of DNA proton resonances could be assigned using a conventional 2D [F1,F2] ^{13}C-filtered NOESY experiment recorded on a ^{13}C/^{15}N DRI-DBD protein bound to unlabeled DNA dissolved in 100% D_2O. A shaded box encloses nucleotides that could not be assigned because their proton resonances are severely broadened in the NMR data of the wild-type complex. (B) Structure of DRI-DBD in the absence of DNA. Regions of the protein that exhibit large changes in their amide chemical shifts as a result of DNA binding are shaded. The location of the Phe355 side chain within the putative DNA binding surface is shown.

(Herrscher et al., 1995; Gregory et al., 1996). The ARID motif adopts a novel 3D structure and is present in a variety of eukaryotic proteins that participate in several biologically significant processes, including global transcriptional activation by the nucleosome remodeling complex SWI/SNF. As a prerequisite for its structural analysis we attempted to completely assign the resonances of the DRI-DBD:DNA complex. Using conventional heteronuclear methods we were able to assign the majority of protein resonances in the complex. However, the application of previously described filtering methods failed to provide NMR data that could be used to assign the duplex. In particular, several proton resonances within base pairs 7–11 of the bound duplex (shaded region in Figure 1A) could not be assigned by the application of a conventional 2D [F1,F2] ^{13}C-filtered NOESY experiment on a DRI-DBD:DNA complex in which the protein was enriched with ^{13}C and ^{15}N and the DNA was unlabeled. Sequence-specific assignments for these nucleotides could not be obtained because their intra- and inter-nucleotide NOE cross peaks were either absent or severely broadened in the 2D [F1,F2] ^{13}C-filtered NOESY spectrum of the DNA. Presumably, resonances from these protons are broadened because their local magnetic environments fluctuate at rates that are intermediate on the chemical shift time scale. In the absence of methods to increase the intensities of these broadened resonances, the structure of the DRI-DBD:DNA complex could not be solved by NMR spectroscopy.

In this paper two approaches have been used to improve the quality of NMR data obtained for the 26 kDa DRI-DBD:DNA complex. First, we present an optimized 2D [F1,F2] ^{13}C-filtered NOESY experiment that incorporates the filtering scheme recently developed by Kay and co-workers (Zwahlen et al., 1997). This experiment enables the observation of NOE cross peaks between ^{12}C- and ^{14}N-bound protons and is more sensitive than previously published

methods. It also can be used in conjunction with a similarly optimized 2D [F2] ^{13}C-filtered NOESY experiment to reliably visualize intermolecular NOEs. Secondly, we demonstrate that in favorable cases it is possible to dramatically improve the NMR spectra of a protein–DNA complex by removing an interfacial aromatic side chain. In particular, we show that a single Phe355Leu mutation within the Dead ringer protein substantially reduces chemical exchange-induced line broadening of its DNA complex, facilitating its detailed investigation by NMR spectroscopy.

Materials and methods

Sample preparation

^{13}C and ^{15}N labeled wild-type and mutated Dead ringer proteins were purified as described previously (Iwahara and Clubb, 1999). The DNA sequence encoding the Phe355Leu mutant protein was generated by PCR and inserted between the BamHI and XhoI restriction sites of the pGEX-4T-1 vector (Pharmacia). The nucleotide sequence of the mutant plasmid was confirmed by DNA sequencing (University of California, Davis sequencing facility). The chemically synthesized DNA fragments for use in the complex (5′-CCTGTATTGATGTGG-3′ and 5′-CCACATCAATACAGG-3′) were purchased from GIBCO Life Technology. Each strand was purified using a MonoQ anion exchange column (Pharmacia) in the presence of 6 M urea to avoid secondary structure formation. Identical amounts of purified complementary oligonucleotides were then mixed, heated to 85 °C, and annealed by slow cooling. The resultant double-stranded DNA fragment was further purified using a MonoQ column under native conditions. The wild-type DRI-DBD:DNA and mutant DRI-DBD^{Phe355Leu}:DNA complexes were formed by mixing equimolar amounts of protein and DNA (80 μM ^{13}C/^{15}N protein and unlabeled DNA dissolved in a buffer consisting of 20 mM Tris HCl, 1 mM EDTA, 1 mM DTT, and 250 mM NaCl). These complexes were then concentrated in a centricon-10 (Amicon) and the buffer was exchanged (NMR buffer: 20 mM Tris-d11 (pH 6.7), 0.01% NaN_3, 0.5 mM EDTA and 5 mM d-DTT, dissolved in 99.996% D_2O). NMR measurements were recorded on ∼1.4 mM wild-type DRI-DBD:DNA and mutant DRI-DBD^{Phe355Leu}:DNA complexes. The amino-terminal domain of the repressor c protein of bacteriophage Mu consists of residues Lys13-Thr81(MUR-DBD). The procedures used to construct the complex have been described previously (Wojciak et al., 2001). The NMR sample of the MUR-DBD:DNA complex was 1 mM in concentration and consisted of equal parts ^{15}N/^{13}C MUR-DBD and an unlabeled DNA 15-mer (NMR buffer: 25 mM phosphate pH 6.2, 2 mM d-DTT, 25 μM EDTA, 0.01% NaN_3 and 99.996% D_2O).

NMR spectroscopy

NMR measurements were performed on a Bruker DRX-600 NMR spectrometer. The sample temperatures were 310 K for the DRI-DBD:DNA complex and 306 K for the MUR-DBD:DNA complex. The parameters of the WURST-20 pulse (Kupce and Freeman, 1995) were set as described by Zwahlen et al. (1997). The pulse was made using the ShapeTool program (Bruker Inc.) and consisted of 1000 points with a maximum RF amplitude of 5 kHz. Its duration was 2.0 ms with a sweep width of 60 kHz and it was swept at a rate of 30.0 MHz s^{-1} from upfield to downfield. The 'purged' filter 2D [F1,F2] ^{13}C-filtered NOESY experiment was run in an identical manner as described by Ikura and Bax (1992). In this experiment the 90° pulses to excite aliphatic and aromatic carbons were applied at 40 ppm and 115 ppm, respectively. For comparison, all experiments were acquired and processed in an identical manner. All data were collected using the following parameters: spectral widths of 6410 Hz in both F1 and F2; mixing times equal to 100 ms; repetition delays equal to 1.1 s; a total of 128 scans per FID; and identical levels of weak presaturation to suppress the HDO signal. Each experiment was acquired for ∼32 h and recorded with a total of 320 and 1024 complex points in the t_1 and t_2 dimensions, respectively. All spectra were processed with a 45° shifted sine bell window function for the t_2 domain and a 60° shifted squared sine bell window function for the t_1 domain. Zero-filling was applied in both dimensions to establish final matrix sizes of 2048 (F2) × 1024 (F1) points. NMR data were processed with the NMRPipe program (Delaglio, 1995) and analyzed with the NMRView program (Johnson and Blevins, 1994).

Results and discussion

A 2D [F1,F2] ^{13}C-filtered NOESY experiment with improved sensitivity

The structural analysis of the unlabeled component of a complex relies heavily upon the interpretation of a

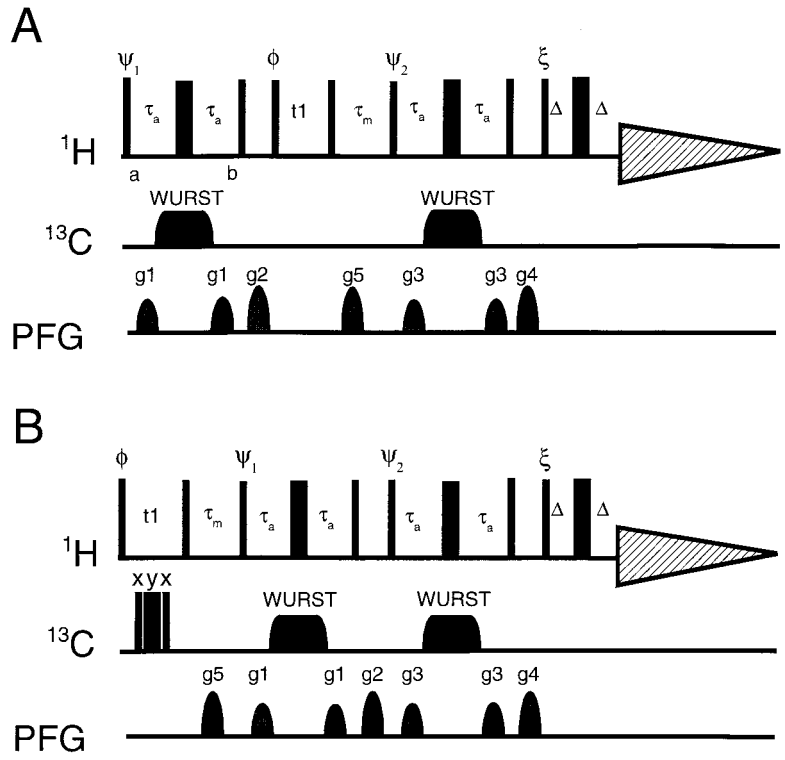

Figure 2. (A) Pulse sequence of the 2D [F1,F2] ^{13}C-filtered NOESY experiment. Rectangular 90° and 180° pulses are represented with thin and bold lines, respectively. Unless indicated, pulse phases are x. The other phases are as follows: $\psi_1 = \{8x, 8(-x)\}$, $\psi_2 = \{16x, 16(-x)\}$, $\phi = \{4x, 4(-x)\}$, $\xi = \{x, y, -x, -y\}$, receiver = {(x, −y, −x, y), 2(−x, y, x, −y), (x, −y, −x, y), (−x, y, x, −y), 2(x, −y, −x, y), (−x, y, x, −y)}. Quadrature detection in the t_1 dimension was accomplished by incrementing phase ϕ in the States-TPPI manner. Delays τ_a and Δ are set to 2.1 ms and 100 μs, respectively. The spin-echo period immediately preceding acquisition (Δ-^{1}H 180° pulse-Δ) is optional and used to obtain better baselines. If this period is omitted, the following receiver phase should be used: {(−x, −y, x, y), 2(x, y, −x, −y), (−x, −y, x, y), (x, y, −x, −y), 2(−x, −y, x, y), (x, y, −x, −y)}. A WURST-20 pulse (Kupce and Freeman, 1995) was utilized and constructed using the 'ShapeTool' in the program XWINNMR (version 2.6, Bruker Instruments, Inc.). The parameters of the pulse were set according to Zwahlen et al. (1997). On a Bruker DRX-600 spectrometer, the sweep width, pulse length, maximum $\gamma B1/2\pi$, and offset of the WURST-20 pulse were 60 kHz, 2.0 ms, 5 kHz, and 0 ppm, respectively. The sweep direction of the WURST-20 was from upfield to downfield. Sine bell shaped gradients were applied along the z-axis with the following strength and duration values: g1 (16 G/cm, 400 μs), g2 (21 G/cm, 900 μs), g3 (16 G/cm, 400 μs), g4 (24 G/cm, 1.1 ms) and g5 (35 G/cm, 2.5 ms). (B) Pulse sequence of the 2D [F2] ^{13}C-filtered NOESY experiment. The parameters for this experiment are identical to (A). The $^{13}C\text{-}90^\circ_x\text{-}180^\circ_y\text{-}90^\circ_x$ composite decoupling pulse was applied at high power ($\gamma B1/2\pi = 18$ kHz) and centered at 65 ppm. Both pulse schemes are designed for samples dissolved in D_2O, because DNA signals under the water line can be visualized and signals from exchangeable DNA protons are eliminated. For samples dissolved in H_2O or for systems that contain slowing exchanging amide protein protons, it is necessary to filter the magnetization of protons attached to nitrogen-15. For cases where only moderate elimination of nitrogen-15 bound proton magnetization is required (samples in D_2O with slowly exchanging amides), nitrogen-180° pulses coincident with the WURST pulses can be applied. For samples recorded in H_2O, where more thorough elimination is required, simultaneous nitrogen-15 and carbon-13 filtration can be implemented as described previously (Zwahlen et al., 1997). However, this latter approach lengthens the overall duration of the 2D [F1,F2] ^{13}C-filtered NOESY experiment, reducing its sensitivity.

2D [F1,F2] ^{13}C-filtered NOESY spectrum, which selectively displays NOE cross peaks originating from ^{12}C- and ^{14}N-bound protons. In order to maximize the intensity of signals arising from ^{12}C-bound DNA protons within the DRI-DBD:DNA complex, we constructed an optimized 2D [F1,F2] ^{13}C-filtered NOESY experiment that incorporates the highly efficient purging scheme recently developed by Kay and co-workers (Zwahlen et al., 1997). The filter in the new experiment was originally presented in the context of a 3D ^{13}C F1-filtered, F3-edited NOESY-HSQC experiment (Zwahlen et al., 1997), but its utility in a 2D [F1,F2] ^{13}C-filtered NOESY experiment has not been previously described. The optimized 2D [F1,F2] ^{13}C-filtered NOESY experiment is presented in Figure 2A and eliminates ^{13}C-bound protons by the application of two pulsed field gradient (PFG) Z-filters that contain frequency swept WURST pulses. Briefly, at step

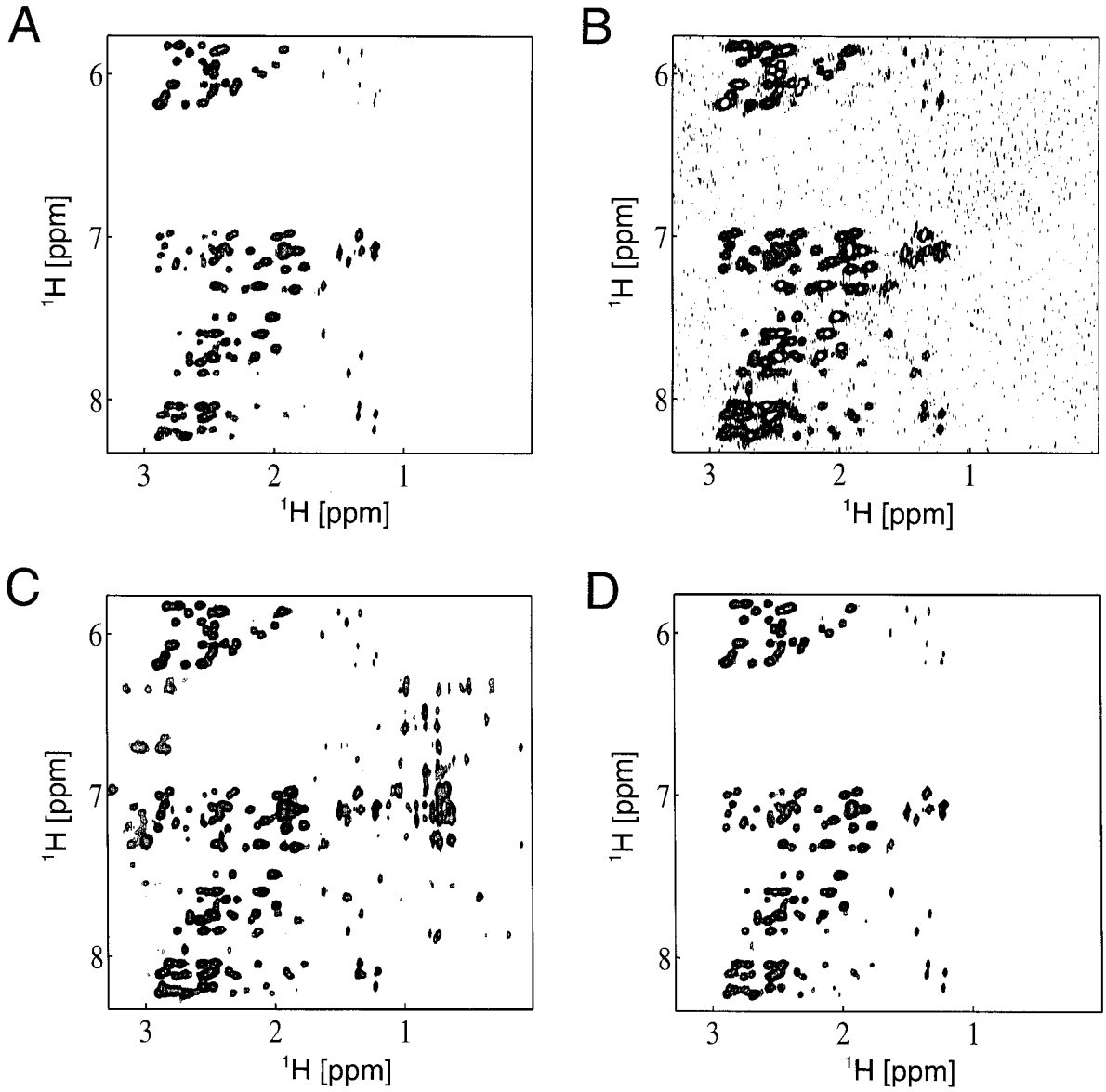

Figure 3. NMR spectra of the DRI-DBD^{Phe355Leu}:DNA complex dissolved in 100% D_2O. (A, B) The WURST optimized 2D [F1,F2] ^{13}C-filtered NOESY spectrum of the DRI-DBD^{Phe355Leu}:DNA complex. Panels (A) and (B) are identical, except that panel (B) has been contoured to show the noise. (C) The ^{13}C decoupled 2D NOESY spectrum of the DRI-DBD^{Phe355Leu}:DNA complex, showing all NOEs (intra-DNA, intra-protein and intermolecular). (D) The 2D [F1,F2] ^{13}C-filtered NOESY spectrum of the complex using a standard 'purged' filter pulse sequence (Ikura and Bax, 1992). All panels show the same region of the NOESY data and were acquired using a 100 ms mixing time.

b, non-^{13}C-attached protons are refocused to in-phase magnetization, while protons attached to ^{13}C are antiphase with respect to one another. The application of the second ^{1}H 90° pulse and subsequent pulse field gradient (g2) dephases the transverse magnetization of the ^{13}C-attached protons, while leaving the longitudinal magnetization of the non-^{13}C-attached atoms unaffected. The filtered magnetization is then subjected to a NOESY pulse sequence and an identical filter is once again applied prior to acquisition.

As described previously, optimal removal of ^{13}C-bound proton magnetization is obtained because the features of the WURST pulse are adjusted to reflect the appropriate $^1J_{HC}$ versus chemical shift profile of

the protein; the WURST pulse has an optimized rate of frequency sweeping, pulse length and maximum field strength (Zwahlen et al., 1997). As a result a single WURST containing unit possesses superb filtering properties, while its overall length is minimized. Figure 3A demonstrates the quality of NMR data obtained when the optimized 2D [F1,F2] ^{13}C-filtered NOESY experiment is performed on a sample consisting of ^{13}C/^{15}N labeled DRI-DBD^{Phe355Leu} (DRI-DBD with a Phe to Leu mutation at position 355) bound to its unlabeled DNA binding site. A comparison of the filtered NOESY spectrum with data obtained from the application of a standard 2D NOESY experiment recorded with ^{13}C decoupling demonstrates the adequate elimination of the ^{13}C-bound proton resonances of the protein (compare Figures 3A and 3C). This is further demonstrated in Figure 3B, which shows only cross peaks between ^{12}C-bound protons, even when the filtered NOESY spectrum is contoured to visualize the noise. A high degree of filtering is critical, because any artifactual NOE cross peaks arising from ^{13}C-bound protons could cause erroneous assignments.

It is important to note that the new sequence should exhibit improved sensitivity as compared to previously described 2D ^{13}C-isotope filtered NOESY pulse schemes that utilize either half-filters (Otting et al., 1986; Otting and Wüthrich, 1989; Folmer et al., 1995; Hyre and Spicer, 1995), purged filters (Gemmecker et al., 1992; Ikura and Bax, 1992), or PFG Z-filters (Ogura et al., 1996). This is because a single WURST PFG Z-filter eliminates ^{13}C-bound proton signals from both aromatic and aliphatic groups, while other protocols that accomplish similar levels of signal filtering are longer in duration. The most commonly used 2D [F1,F2] ^{13}C-filtered NOESY experiment eliminates ^{13}C- and ^{15}N-bound proton magnetization by converting it to undetectable multiple-quantum coherence (Ikura and Bax, 1992). We directly compared this older sequence to the WURST optimized pulse program by performing each experiment on the DRI-DBD^{Phe355Leu}:DNA complex using identical experimental conditions (same recycle times, number of scans, and data points in the t_1 and t_2 dimensions). Although both experiments exhibit similar filtering efficiencies (compare Figures 3A and 3D), there is a marked improvement in the intensities of the NOE cross peaks in the spectrum obtained using the WURST optimized pulse sequence. For resolved NOE cross peaks in the DRI-DBD^{Phe355Leu}:DNA complex there is a 28.9±17.1% average improvement in the signal intensities when the WURST sequence is em-

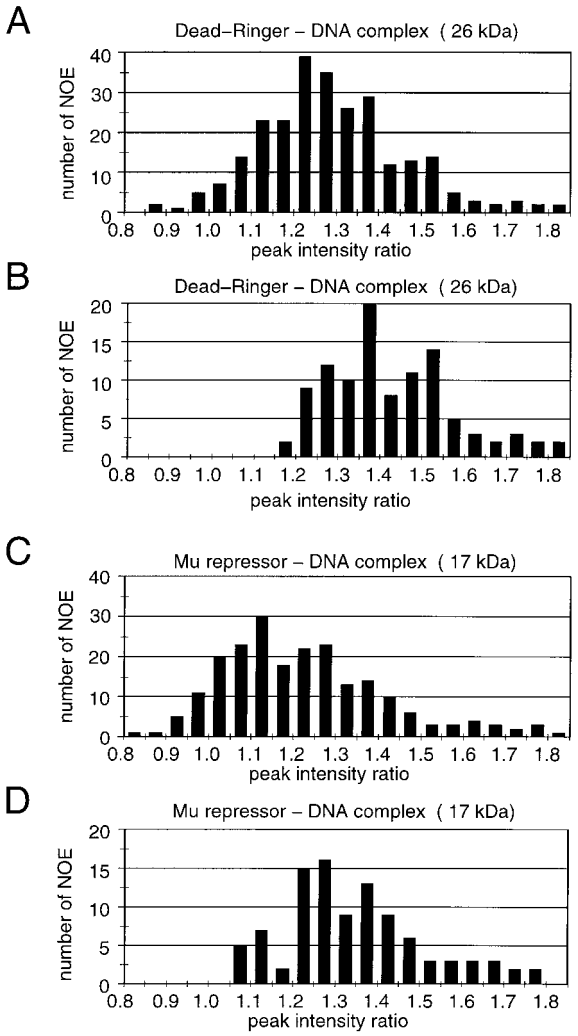

Figure 4. Histograms that compare the cross-peak intensities within the WURST optimized (Figure 2A) and 'purged' filtered 2D [F1,F2] ^{13}C-filtered NOESY spectra. Bars represent the ratio of the cross-peak intensities in the two spectra (WURST optimized/conventional approach). For comparison both experiments were run in an identical manner. (A) and (B) compare the performance of these pulse programs when applied to the DRI-DBD^{Phe355Leu}:DNA complex dissolved in 100% D_2O. Panel (A) shows the ratios of all resolved cross peaks and panel (B) shows the ratios of all resolved cross peaks involving H2′ or H2″ atoms. Panels (C) and (D) show a comparison of the pulse programs when applied to the MUR-DBD:DNA complex dissolved in 100% D_2O. Panel (C) shows the ratios of all resolved cross peaks and panel (D) shows the ratios of all resolved cross peaks involving H2′ or H2″ atoms. We note that a fewer number of cross peaks were used in the analysis of MUR-DBD:DNA complex data, since the number of resolved cross peaks in this system is substantially lower than that of the DRI-DBD^{Phe355Leu}:DNA complex.

ployed (Figure 4A). This sensitivity gain can be attributed to a 4.8 ms reduction in the time in which proton magnetization is transverse in the WURST containing sequence as compared to the 2D [F1,F2] ^{13}C-filtered NOESY that employs the 'purged' filter (Ikura and Bax, 1992) (WURST optimized, 8.4 ms; 'purged' filter, 13.2 ms). If it is assumed that the cross peak intensity differences are solely a result of transverse proton relaxation during this additional period, sensitivity gains between ∼10–49% are expected for NOE cross peaks involving protons that have T_2 values ranging between 50 and 12 ms. This is consistent with the observed 42.8±14.9% intensity increase in NOE cross peaks involving the H2′ and H2″ protons of the DNA (Figure 4B), since dipolar interactions between these proximal protons cause their rapid relaxation. The sensitivity improvement of cross peaks involving H2′/H2″ protons is significant, since NOEs between the H6/H8 atoms of the bases and the H2′/H2″ protons of the ribose rings play a critical role in conventional nucleotide assignment protocols (Wüthrich, 1986).

The performance of the WURST optimized sequence was also assessed using a different protein–DNA complex for which complete resonance assignments and a three-dimensional solution structure are known (Wojciak et al., 2001). This complex consists of ^{13}C/^{15}N labeled Mu repressor DNA-binding domain and an unlabeled 15-bp duplex (MUR-DBD:DNA, 17 kDa). Figures 4C and 4D display histograms of the NOE cross-peak intensity ratios of data recorded on the MUR-DBD:DNA complex using the WURST optimized and the 'purged' filter scheme. On average there is a 22.1±19.3% increase in the intensities of well-resolved NOE cross peaks (Figure 4C), while the intensities of cross peaks involving the H2′ and H2″ atoms are increased by 34.5±16.7% (Figure 4D).

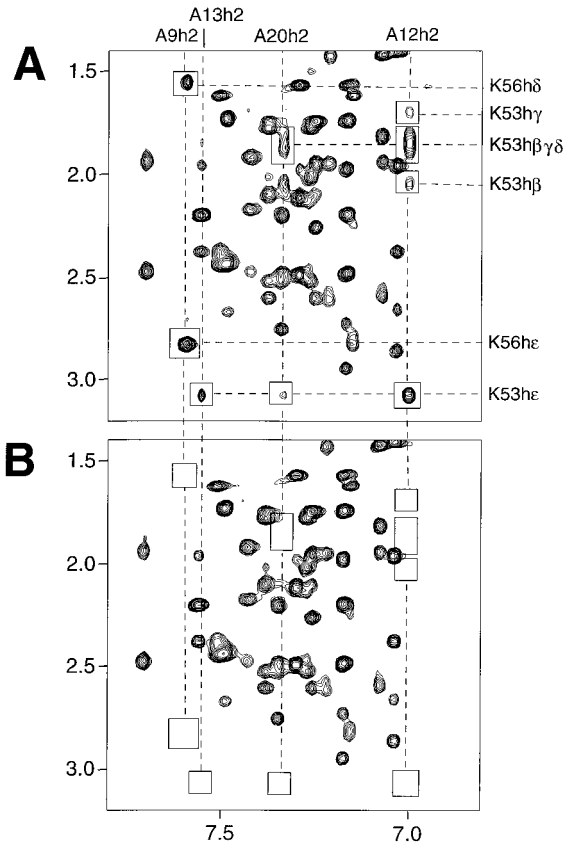

Figure 5. (A) 2D [F2] ^{13}C-filtered NOESY and (B) [F1,F2] ^{13}C-filtered NOESY spectra of the MUR-DBD:DNA complex. The data sets were recorded using the pulse programs in Figure 2 under identical experimental conditions. In panel (A) cross peaks enclosed by boxes correspond to protein–DNA intermolecular NOEs and are labeled. For comparison, the same regions in panel (B) are also enclosed in boxes.

A complementary experiment to identify intermolecular NOEs

It has previously been shown that comparing F2- and F1, F2-filtered 2D NOESY spectra is a particularly useful method to detect intermolecular NOEs (Fesik et al., 1991; Weber et al., 1991). We therefore constructed a complementary WURST optimized 2D [F2] ^{13}C-filtered NOESY experiment (Figure 2B) that displays intra-DNA cross peaks plus intermolecular NOEs between the protein and DNA. It is important to note that the data obtained from the pulse sequences in Figure 2 are directly comparable, since in each, the proton magnetization is transverse for an identical amount of time. In our experience we have found these two 2D experiments to be complementary to 3D ^{13}C F1-filtered, F3-edited NOESY-HSQC data, which displays intermolecular NOEs edited by the frequency of the attached ^{13}C atom (Zwahlen et al., 1997). First, the intensities of intermolecular cross peaks tend to be greater in the 2D [F2] ^{13}C-filtered NOESY spectrum as compared to the 3D ^{13}C F1-filtered, F3-edited NOESY-HSQC spectrum, allowing weak intermolecular NOEs to be identified. Second, comparison of the complementary 2D experiments enables the rapid identification of intermolecular NOEs and thus serves as an excellent first screen for determining whether a particular protein–DNA complex warrants further analysis. Third, potential artifactual NOEs are expected to appear with equal intensity in

both the 2D F1, F2-filtered and F2-filtered NOESY spectra, such that there is little danger that they will be miss-assigned as intermolecular contacts. Finally, the intensities of intermolecular NOEs in the 2D [F2] ^{13}C-filtered NOESY spectrum can be directly calibrated with respect to NOE cross peaks arising from the DNA. This enables increased accuracy in the classification of intermolecular distance restraints, facilitating greater definition of the protein–DNA interface.

The utility of the complementary 2D experiments is demonstrated in Figure 5, which displays the spectra of the fully assigned MUR-DBD:DNA complex recorded with either the 2D [F2] ^{13}C-filtered NOESY (Figure 5A) or the [F1,F2] ^{13}C-filtered NOESY (Figure 5B) experiments. A comparison reveals the presence of additional cross peaks in the [F2] ^{13}C-filtered NOESY spectrum, which can be attributed to intermolecular NOEs between the DNA and the protons of Lys53 and Lys56 (regions enclosed by boxes). In particular, there are numerous cross peaks between the side chains of these residues and the adenine H2 protons within the minor groove.

Improved complex spectra through the targeted replacement of an interfacial aromatic side chain

Although the WURST optimized 2D [F1,F2] ^{13}C-filtered NOESY experiment shows improved sensitivity, extensive resonance line broadening in the spectrum of the DRI-DBD:DNA complex remained. For example, several of the intra- and inter-nucleotide NOEs between the H6/H8 and H2′/H2″ protons in the NOESY data of the DRI-DBD:DNA complex were broadened (Figure 6A, boxed regions marked ‘a’ and ‘b’). Presumably these signals are broadened by slow time scale dynamics between non-magnetically equivalent conformers of the complex that result from either its complete dissociation or by more local time dependent changes within the interface. For a two-site model the contribution of chemical exchange to the transverse relaxation rate is proportional to the square of the chemical shift difference between the exchanging species. This suggests that the removal of interfacial side chains that significantly alter the magnetic environments of proximal nuclei could in principle sharpen resonances at the molecular interface. Since aromatic rings cause large ring-current-induced perturbations in the chemical shifts of proximal nuclei, we inspected the DNA binding surface on DRI-DBD for these types of amino acids. The contact surface on DRI-DBD was previously mapped from an analysis of the chemical shift perturbations that result from DNA binding, and by modeling studies of the protein–DNA complex. Inspection of this surface revealed the presence of a single aromatic side chain, Phe355, which was subsequently mutated to a leucine residue to construct DRI-DBD^{Phe355Leu}. The 2D ^{1}H-^{15}N HSQC spectrum of the ^{15}N labeled DRI-DBD^{Phe355Leu} mutant indicated that it adopts a similar three-dimensional structure as the wild-type protein and band-shift analysis revealed that it retained affinity for DNA (data not shown). Most importantly, the mutant DRI-DBD^{Phe355Leu}:DNA complex exhibits a similar pattern of intra- and intermolecular NOEs, strongly suggesting that both its structure and mechanism of binding are closely related to the wild-type complex.

A comparison of the mutant and wild-type 2D [F1,F2] ^{13}C-filtered NOESY spectra reveals that the mutant exhibits both improved line shape and an increase in the total number of NOE cross peaks (compare Figures 6A and 6B). For example, cross peaks between the H6/H8 and H2′/H2″ protons are sharpened in the mutant complex (compare boxed regions denoted ‘a’ and ‘b’ in Figures 6A and 6B). There is also a general increase in the number of observable intramolecular NOE cross peaks in the DNA spectrum of the mutant complex (compare boxed regions denoted ‘c’ to ‘f’ in Figures 6A and 6B). The superior quality of the spectra of the DRI-DBD^{Phe355Leu}:DNA complex is further demonstrated in Figure 7, which displays NOE cross peaks between the methyl and H6 protons of the thymine bases in the absence of protein (Figure 7A), in the wild-type DRI-DBD:DNA complex (Figure 7B), and in the DRI-DBD^{Phe355Leu}:DNA complex (Figure 7C). In the absence of protein, a series of well-defined NOE cross peaks correlate the methyl and H6 protons of the eight thymine bases within the duplex (Figure 7A). However, in the wild-type complex these cross peaks are broadened, preventing the unambiguous assignment of resonances from thymines 8 and 21. Strikingly, the 2D [F1,F2] ^{13}C-filtered NOESY spectrum of the mutant complex exhibits excellent spectral resolution and line shape, enabling its complete assignment (compare Figures 7B and 7C).

An obvious problem with the targeted mutagenesis approach is that the mutated protein may exhibit weaker affinity for its ligand or be less stable. It is thus important that aromatic residues targeted for replacement be altered in a conservative manner and that they not participate in extensive protein stabilizing interactions. In the case of the Dead ringer protein, the side

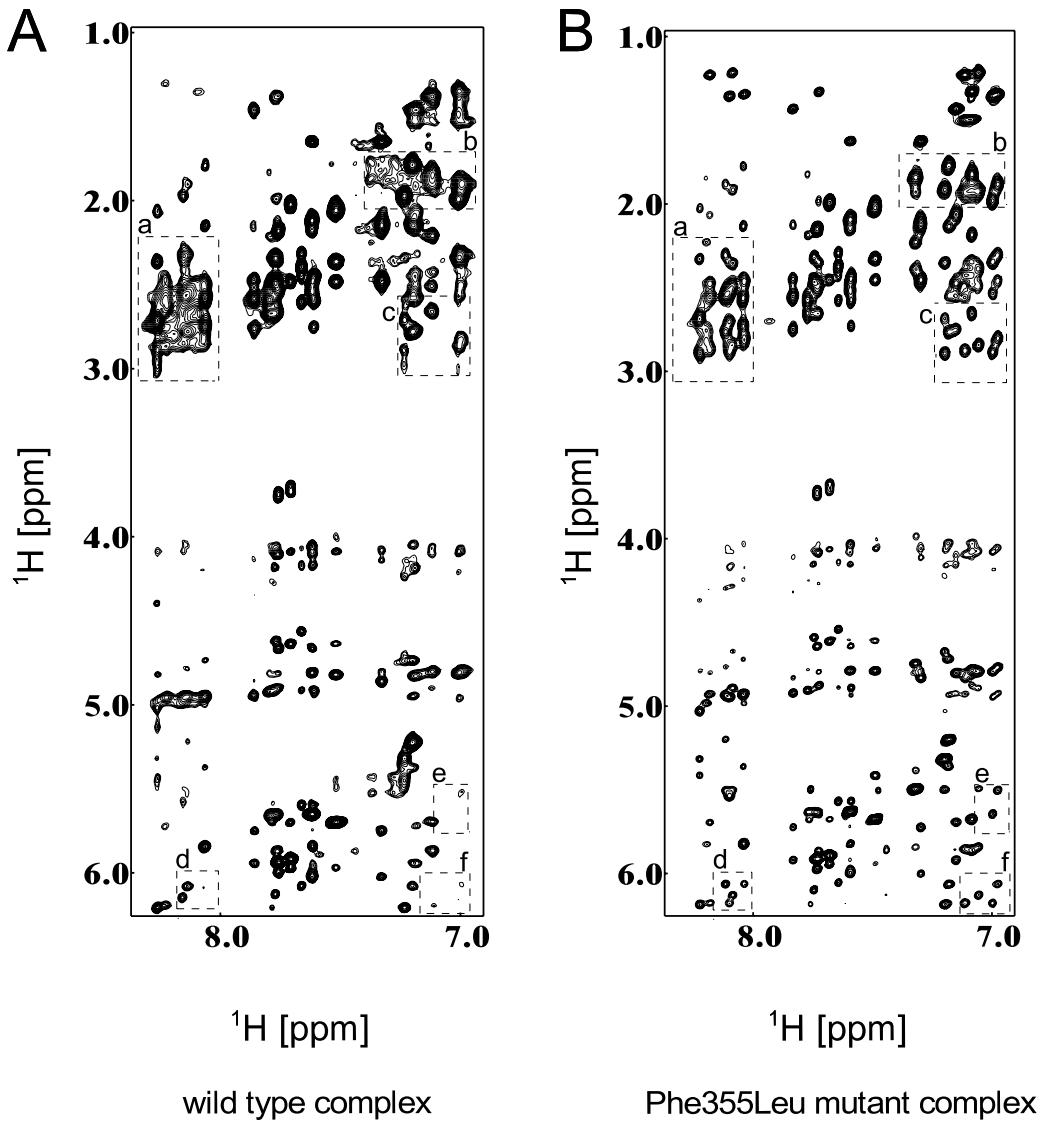

Figure 6. Comparison of the NMR spectra of the wild-type DRI-DBD:DNA and DRI-DBD^{Phe355Leu}:DNA complexes dissolved in 100% D_2O. Each panel shows identical regions of the 2D [F1,F2] ^{13}C-filtered NOESY spectrum of (A) the wild-type DRI-DBD:DNA complex and (B) the DRI-DBD^{Phe355Leu}:DNA complex. Regions of the spectra that are improved by the Phe355Leu mutation are enclosed within boxes.

chain of Phe355 is positioned on the protein surface and does not play a role in stabilizing the structure. Moreover, its conservative replacement with leucine causes only an approximate twofold reduction in affinity for DNA as judged by band-shift analysis (data not shown). This is consistent with the idea that conservative amino acid substitutions are unlikely to cause large reductions in affinity and specificity, especially when placed within the context of a large binding surface formed by several amino acids. It should further be noted that most NMR studies of macromolecular complexes are performed at millimolar sample concentrations, which are several orders of magnitude higher than the dissociation constant of a typical complex (10^{-9} to 10^{-7} M). This suggests that even mutants with substantially reduced affinities will form complexes that are highly populated at the concentrations used for NMR. The removal of phenylalanine side chains appears to have the greatest chance of success, because this side chain does not donate or accept hydrogen bonds. We chose a phenylalanine to leucine mutation, because both are non-polar and branched

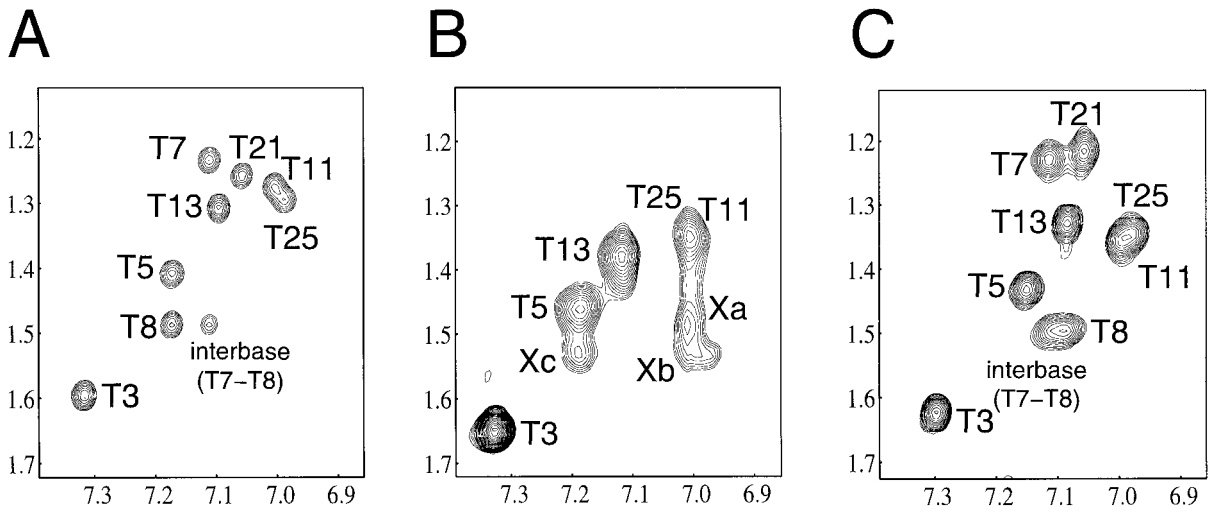

Figure 7. The effects of wild-type and mutant protein binding on the NOESY spectrum of the bound DNA molecule. (A) 2D NOESY spectrum of the protein-free DNA. Except where labeled, all cross peaks correspond to the intrabase NOEs between the H6 and C5 methyl protons. (B, C) The 2D [F1,F2] ^{13}C-filtered NOESY spectra of the wild-type DRI-DBD:DNA complex and the mutant DRI-DBD^{Phe355Leu}:DNA complex. All spectra were acquired using a 100 ms mixing time. Xa, Xb and Xc denote unassigned cross peaks.

at their Cγ carbons. Replacement of histidine, tryptophan, and tyrosine side chains may prove more problematic, because they can form hydrogen bonds to the duplex. Replacement with either non-polar (e.g. alanine or valine) or polar long chain aliphatic side chains (e.g. glutamine) may prove successful. There are numerous NMR studies of protein-containing complexes that report resonance line-broadening, which is generally attributed to exchange that is intermediate on the chemical shift time scale. The extent to which these deleterious exchange effects can be attributed to the motion of interfacial aromatic side chains is unknown. However, it is encouraging to note that a recent review of high resolution atomic structures of protein–DNA and protein–protein complexes revealed that aromatic residues comprise 11.5% and 21.6% of their interaction surfaces, respectively (Lo Conte et al., 1999; Nadassy et al., 1999), suggesting that, although not a general method, targeted removal of interfacial aromatic side chains may prove to be useful in the spectral optimization of other protein-containing complexes. Finally, we note that the replacement of aromatic side chains with methyl-containing amino acids may significantly increase the number of observable intermolecular NOEs, because methyl protons have favorable NMR properties. For example, in the DRI-DBD^{Phe355Leu}:DNA complex we have identified numerous intermolecular NOEs from the Hδ methyl protons of Leu355, suggesting that the structure of this region of the interface can now be accurately defined.

Conclusions

We have demonstrated the utility of two methods, one biochemical and one spectroscopic, both of which increase the quality of NMR spectra obtained for a protein–DNA complex. First we have shown that a minor modification of the 2D [F1,F2] ^{13}C-filtered NOESY experiment substantially increases its sensitivity as compared to previously published pulse schemes (up to 40% in favorable cases). We also have demonstrated that the 2D [F1,F2] ^{13}C-filtered NOESY experiment, in combination with a complementary 2D [F2] ^{13}C-filtered NOESY experiment, provides a valuable method to identify intermolecular NOEs. Although the utility of these experiments has been demonstrated on two protein–DNA complexes, they should prove useful in the study of any complex consisting of a ^{13}C/^{15}N enriched protein and an unlabeled ligand. In addition, we have shown that in favorable cases line broadening within the spectra of a protein–DNA complex can be reduced by removal of an interfacial aromatic side chain. The changes in the spectra are dramatic, salvaging a protein–DNA complex that was originally ill suited for structural analysis by NMR. Previous NMR studies have attributed interface line broadening effects to entropically advantageous fluctuations in the network of protein–DNA hydrogen bonds (Billeter et al., 1993; Foster et al., 1997). Our results suggest that interface line broaden-

ing can also arise from dynamic changes in proximal aromatic rings.

Acknowledgements

We thank Dr. Robert Peterson for technical support. This work was supported by a grant from the US Department of Energy (DE-FC-03-87ER60615).

References

Billeter, M., Qian, Y.Q., Otting, G., Müller, M., Gehring, W. and Wüthrich, K. (1993) *J. Mol. Biol.*, **234**, 1084–1093.

Clore, G.M. and Gronenborn, A.M. (1998) *Trends Biotechnol.*, **16**, 22–34.

Delaglio, F., Grzesiek, S., Vuister, G.W., Zhu, G., Pfeifer, J. and Bax, A. (1995) *J. Biomol. NMR*, **6**, 277–293.

Fesik, S.W., Gampe, R.T., Eaton, H.L., Gemmecker, G., Olejniczak, E.T., Neri, P., Holzman, T.F., Egan, D.A., Edalji, R., Simmer, R., Helfrich, R., Hochlowski, J. and Jackson, M. (1991) *Biochemistry*, **30**, 6574–6583.

Folmer, R.H.A., Hilbers, C.W., Konings, R.N.H. and Hallenga, K. (1995) *J. Biomol. NMR*, **5**, 427–432.

Foster, M.P., Wuttke, D.S., Radhakrishnan, I., Case, D.A., Gottesfeld, J.M. and Wright, P.E. (1997) *Nat. Struct. Biol.*, **4**, 605–608.

Gemmecker, G., Olejniczak, E.T. and Fesik, S.W. (1992) *J. Magn. Reson.*, **96**, 199–204.

Gregory, S.L., Kortschak, R.D., Kalionis, B. and Saint, R. (1996) *Mol. Cell. Biol.*, **16**, 792–799.

Herrscher, R.F., Kaplan, M.H., Lelsz, D.L., Das, C., Scheuermann, R. and Tucker, P.W. (1995) *Genes Dev.*, **9**, 3067–3082.

Hyre, D.E. and Spicer, L.D. (1995) *J. Magn. Reson.*, **B108**, 12–21.

Ikura, M. and Bax, A. (1992) *J. Am. Chem. Soc.*, **114**, 2433–2440.

Iwahara, J. and Clubb, R.T. (1999) *EMBO J.*, **18**, 6084–6094.

Johnson, B.A. and Blevins, R.A. (1994) *J. Biomol. NMR*, **4**, 603–614.

Kupce, E. and Freeman, R. (1995) *J. Magn. Reson.*, **A117**, 246–256.

Lo Conte, L., Chothia, C. and Janin, J. (1999) *J. Mol. Biol.*, **285**, 2177–2198.

Nadassy, K., Wodak, S.J. and Janin, J. (1999) *Biochemistry*, **38**, 1999–2017.

Ogura, K., Terasawa, H. and Inagaki, F. (1996) *J. Biomol. NMR*, **8**, 492–498.

Otting, G., Senn, H., Wagner, G. and Wüthrich, K. (1986) *J. Magn. Reson.*, **70**, 500–505.

Otting, G. and Wüthrich, K. (1989) *J. Magn. Reson.*, **85**, 586–594.

Weber, C., Wider, G., Vonfreyberg, B., Traber, R., Braun, W., Widmer, H. and Wüthrich, K. (1991) *Biochemistry*, **30**, 6563–6574.

Wojciak, J.M., Iwahara, J. and Clubb, R.T. (2001) *Nat. Struct. Biol.*, **8**, 84–90.

Wüthrich, K. (1986) *NMR of Proteins and Nucleic Acids*, John Wiley and Sons, New York, NY.

Zwahlen, C., Legault, P., Vincent, S.J.F., Greenblatt, J., Konrat, R. and Kay, L.E. (1997) *J. Am. Chem. Soc.*, **119**, 6711–6721.